High Peak Power Tapered RWG Laser Diodes for Eye-Safe LIDAR Applications Around 1.5 µm Wavelength

Topi Uusitalo*, Jukka Viheriälä, Heikki Virtanen, Santeri Hanhinen, Roosa Hytönen, Jari Lyytikäinen, Mircea Guina
Optoelectronics Research Centre/Physics, Tampere University, Korkeakoulunkatu 3, FI-33720 Tampere, Finland

ABSTRACT

High peak power and brightness eye-safe lasers are desired in automotive LIDAR, for example. We address this need by developing tapered ridge waveguide lasers with highly asymmetric InGaAsP/InP epilayer emitting at around 1.5 µm wavelength. The structure allows state-of-the-art peak power of 7.3 W at 50 A current. Preliminary beam quality results indicate that the epi-design enables higher beam brightness than more traditional structures when driven with high amplitude current pulses. Results indicate that further improvements in power and brightness characteristics are possible with more optimized cavity layout and laser driver design.

Keywords: Semiconductor laser, tapered laser, LIDAR, pulsed laser

1. INTRODUCTION

High peak power ns-scale pulsed laser light is desired in e.g. time-of-flight (ToF) LIDAR applications [1]. Additionally, the beam quality of the high-power source determines how far the light source is usable. For practical applications, the size, weight, power, and cost (SWaP-C) are also important, especially for consumer grade applications, for example in autonomous vehicles. Finally, if the usage scenarios include people or other beings with biological vision, it is of utmost importance to consider the eye-safety of the used sources.

Currently state-of-the-art power levels for LIDAR laser diodes are obtained at around the “9xx” nm range. More than 50 W wavelength locked output was realized in [2] from a 100 µm wide emitter. Around 18 W, but nearly diffraction limited output was achieved from an emitter with a tapered geometry [3]. More than 460 W is reported from a stacked quantum well epilayer design 800 µm wide [4]. The other wavelength range is at around 1.5 µm, where eye safety power levels (maximum permissible exposure) are up to 5 orders of magnitude higher (IEC 60825). A similar epilayer design as employed in this publication has been used to obtain 18 W from 90 µm wide emitter at this eye-safe wavelength range [5].

We have developed a source that combines most of the criteria for ToF LIDAR sources. High peak power is achieved with a specialized epilayer structure, the beam quality is addressed by various tapered designs, SWaP-C is intrinsic as the sources are direct emission laser diodes and last the eye-safety levels are very high for emitters in the used wavelength range of 1.5 µm, especially when short pulse lengths are used: permitted peak power level is approximately inversely proportional to the used pulse width.

This paper is structures as follows. In section 2, the used epitaxial structure and lateral device designs are introduced. The used measurement methods are covered in section 3, and in section 4 the achieved results are analyzed. Finally, the paper is summarized in section 5.

*topi.uusitalo@tuni.fi

2. DEVICE DETAILS

2.1 Epitaxial structure

The epitaxial structure of the lasers uses a bulk gain layer, asymmetric cladding compositions and a thin p-side waveguide layer. These factors lead to an asymmetric nearfield intensity distribution, which has a low overlap with the p-doped side. In addition, the thin p-side waveguide leads to low carrier accumulation, and together with the bulk gain layer, they lead to high peak and saturation power levels. A more detailed discussion on the epitaxial structure is given elsewhere [6]–[8]. A reference design that used a symmetrical multiple quantum well (MQW) epilayer structure with a comparable QW confinement factor Γ was used to confirm the improvement provided by the used bulk epilayer design. This reference design was used previously to obtain up to 4.6 W pulsed peak power with a narrow spectrum from a tapered Bragg reflector laser diode [9].

2.2 Ridge and taper design

A transversely single-mode ridge waveguide (RWG) was used to get a good input beam quality for the used taper sections. The index guiding RWG was defined by etching 12 µm wide trenches to the semiconductor. A more detailed description on the manufacturing of similar lasers is given in [9]. The ridge width was fixed to 1.5 µm in all the fabricated device variants. This width was determined to give the best far-field distribution and kink-free LI-curve in a test process. The taper sections had the RWG as an input and the two sections had either common or separate openings. The longitudinal spacing of the separate contacts was in the range $30 - 60$ µm. Tapers with different opening angles (θ), 1, 3, and 6 degrees, were fabricated. The taper was defined by the contact opening and there was no index guiding at the lateral sides of the tapers. A sketch of the use TRWG geometry is shown in the left panel of Figure 1.

3. MEASUREMENT METHODS

The lasers were measured in pulsed mode with two different ns pulse drivers. First, HLD500 from Dr. Heller, capable of pulse lengths in the range 30-160 ns, with up to 50 A amplitude. The other driver was a LIDAR test board EPC9126 from EPC, capable of 3 ns long 75 A pulses. In practice the maximum current amplitude was limited to 50 A due to series inductance of the used setup. The laser diodes were mounted on gold-plated SiN submounts, and the mounted lasers were contacted to the pulse drivers with pogo-pin style contacts. A broad area laser was measured in a minimal inductance configuration with the EPC9126 and 75 A pulses were achieved. These high amplitude pulses were not, however, possible for the lasers mounted on submounts due to additional contacting pins required in the configuration.

The lasers were first measured for light-current (LI) characteristics. In the ns-pulse domain the measurement is two-staged: first the average power is measured with an integrating sphere power detector and subsequently the time trace of the pulse is measured with a fast photodiode (5 GHz Thorlabs DET08CL/M, 70 ps rise time) and an oscilloscope. The amplitude and area of the pulse with the repetition rate and average power are used to convert the average power to pulse peak power.

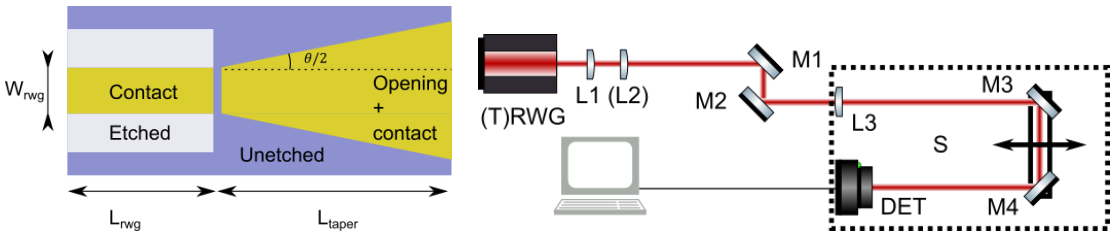

Figure 1. Left: Sketch of the general layout of the studied TRWGs. Right: The measurement setup used for M2 measurement. (T)RWG: (Tapered) ridge waveguide laser; L1-3: lenses, aspheric collimation lens, acylindrical collimation lens, plano-convex collimation lens; M1-M4: planar mirrors; S: scanning stage with a 100 mm travel range, Thorlabs M2MS; DET: beam detector, Thorlabs BP209-IR2 scanning slit camera.

The beam quality of a laser beam can be measured by scanning the beam diameter around a waist. Here a scanning slit detector was used in a max-hold mode to collect the mode shapes of the pulsed source, which was pulsed at a low frequency (5 kHz). The low frequency implies that the whole beam shape is not measured with one rotation of the drum in the scanning slit detector, but rather the beam is effectively spatially sampled, thus the max-hold mode was required. The beam shape was considered fully measured when the sum of L2-norms of the difference between several sequential measurements dropped below a setpoint, and the longitudinal scanning was automated. The beam width was determined

as the $1/e^2$ width, as per ISO11146-3. The 4σ width cannot be used with scanning slit cameras, because only two axes of the mode are measured. The sum of L2 norms was calculated according to

$$\boldsymbol{A} = \sum_{\boldsymbol{j=M-K+1}}^{\boldsymbol{M}} \|\boldsymbol{x_{N-1}} - \boldsymbol{x_N}\|_{\boldsymbol{2,j}}, \quad (1)$$

where x_N and x_{N-1} are the two latest light intensity traces from the detector operating in the max hold mode acquired to memory at a point of time j. The acquisition of summed L2 norm is stopped at a point of time M, when the value A is compared a setpoint. K number of L2 norm values are considered in the sum. Due to the asynchronous nature of the algorithm, the time points N and $N-1$ are not necessarily adjacent between sequential L2 evaluations j. When $A = 0$, no further higher beam intensity points were measured in the K points. In practice, a much higher value of A was usable as the setpoint without affecting measurement accuracy.

The measurement procedure of the beam quality was the following for the RWG lasers. The beam was collimated with lens L1 (LightPath Technologies 355330C aspherical lens, NA $= 0.77$, f $= 3.1$ mm) and aligned with the measurement stage S and the scanning slit detector DET. The scanning slit was rotated so that the elliptical beam was aligned with the detector slits. The beam was subsequently focused to approximately the center of the measurement range by a f $= 250$ mm plano-convex AR-coated lens L3. The beam width was then measured at several points around the waist, and those measurements used to fit the beam caustic with a nearly Gaussian beam with $M_2 \geq 1$.

The tapered RWG laser (TRWG) is an astigmatic source and a second lens, acylindrical L2 (asphericon CHL18-15-S f $=$ 15 mm), was used to collimate the lateral direction. It was noted that the rotation angle causes errors in the M_2 measurement even with small misalignments. Thus, L2 was rotated in the same manner as DET to align the beam with the optical components. Because the beam quality in the two beam axes were somewhat different, the waist positions from the focusing lens differed. It was determined that a plano-convex lens with f $= 150$ mm as L3 was appropriate to have the waists of both axes within the measurement range. The measurement setup is summarized in the right panel of Figure 1.

4. RESULTS AND DISCUSSION

Laser diodes of various geometries were characterized for this publication. The measured device IDs and descriptions are compiled in Table 1. The devices with two contacts have separated contact openings on the RWG and taper parts of the devices. These contacts have been, however, shorted, and consequently the same current pulses are applied to both contacts.

Table 1. Summary of the measured device variants. Variants A and E are oxide stripe and RWG, respectively.

Device ID	Gain type	W_{rwg} (μm)	L_{rwg} (mm)	L_{taper} (mm)	θ(°)	No. of contacts
A	bulk	80	2	-	-	1
B	bulk	1.5	1	4	1	1
C	bulk	1.5	1	4	1	2
D	bulk	1.5	1	2	3	2
E	bulk	1.5	1	-	-	1
F	MQW	2.5	1	2	3	2

4.1 LI characteristics

The LI curves were measured from various device geometries, and the results are compared in Figure 2. The tapered RWG lasers show at most 88 % maximum peak power compared to the total output from an oxide stripe. This penalty is partially attributed to absorbing sections between the RWG and taper sections, and the taper and the facet, partially to optical losses from e.g. the coupling between the RWG and the taper and to the possible differences in injection efficiency. A clear kink at the threshold current is seen in several of the measured TRWG devices. We attribute this to the unpumped region between the RWG and taper sections, where the absorption is saturated. The effect is visible with both variants C (30 µm

unpumped region) and D (60 µm unpumped region). This effect was further studied by varying the applied current pulse length to variant D. The result is shown in Figure 4. Elongating the pulse smoothens out the kink and decreases the threshold current to about 60 %. This agrees with results from saturable absorber lasers using similar pumping scheme [10]. At longer pulses the threshold current starts to slightly increase, which we attribute to thermal load experienced by the laser during the pulses.

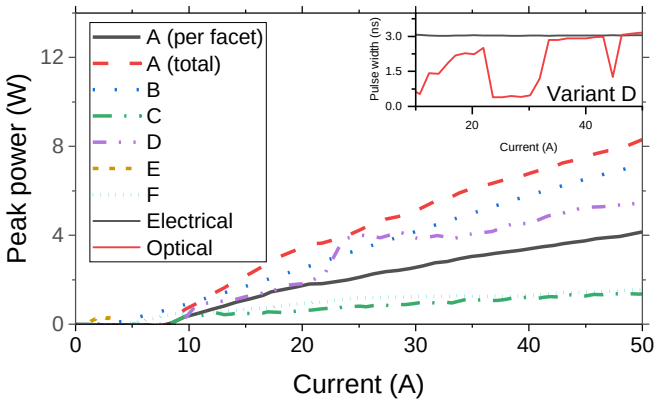

Figure 2. Measured LI curves from various device geometries. A: bulk gain broad area laser B: bulk gain 4 mm long taper with 1 degree total opening and common contacts of RWG and taper; C: bulk gain 4 mm long taper with 1 degree total opening and separate contacts; D: bulk gain 2 mm long taper with 4 degree opening and separate contacts; E: bulk gain 2 mm long RWG; F: QW gain 2 mm long taper with 3 degree total opening and separate contacts. All traces measured with 3 ns long pulses, except for B which used 50 ns pulse length. The pulse width of variant D is shown in the inset.

The injection circuitry was kept at constant 3 ns pulse width setting for all the measurements in Figure 2. The pulse width variation of variant D is shown in the inset of the figure. Near the threshold, a narrow pulse emerges, which then starts to broaden as lasing threshold is reached by subsequent pulses. There is another absorption mechanism, which emerges at 24 A injection current. It absorbs parts of the pulse, narrowing its width to the initial value. However, the absorption is also experienced by the main pulse, as the peak power stays constant. After the pump pulse amplitude increases sufficiently, the pulse width returns to follow that of the electrical pulse. The used photodetector had a rise/fall times close to the shortest measured pulse. This may lead to small errors in the peak power measurement in the short pulse regimes, but the peak powers are relatively close between short and long pulse regimes, so we assume the possible error to be small.

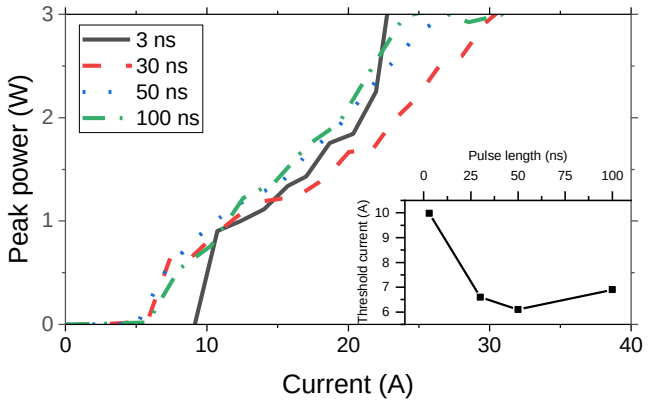

Figure 3. Measured LI of device D with varying pulse length. The effect of saturation diminishes with increasing pulse length, and the threshold current drops by almost 40 %, as shown in the inset.

4.2 Beam quality results

A tunable pulse length source (HLD500) was used to study the effect of pulse length to the measured beam quality. The resulting caustics are shown in Figure 4, where it is seen that the beam waist diameter, and, consequently, the M^2, increases with the pulse length when all the measurement optics remain unchanged between measurements. The peak power level

at a constant current amplitude of 20 A stays within a 25 % range and its dependence to pulse length is not monotonous, hence it cannot explain the variation in the beam quality. The degradation effect can be due to a changing temperature gradient inside the laser during the sub-µs pulses. There is, however, at least the carrier density induced anti-guiding effect inside the gain-guided taper section which has an effect on the beam quality. It has an opposite effect to the current pulse induced thermal gradient, which can lead to positive guiding or thermal lensing [11]. The impact of these effects to e.g. the astigmatism was beyond the measurement accuracy used in this paper. The beam quality was also measured in the short pulse regime (e.g. variant D with 25 A current), but there was no discernable effect compared to the longer (3 ns) pulse regimes. Studying the combined effect is planned in future work. Because of the improvement in beam quality, a shorter pulse length driver was subsequently used, and the M_2 value improved significantly, as also shown in the figure.

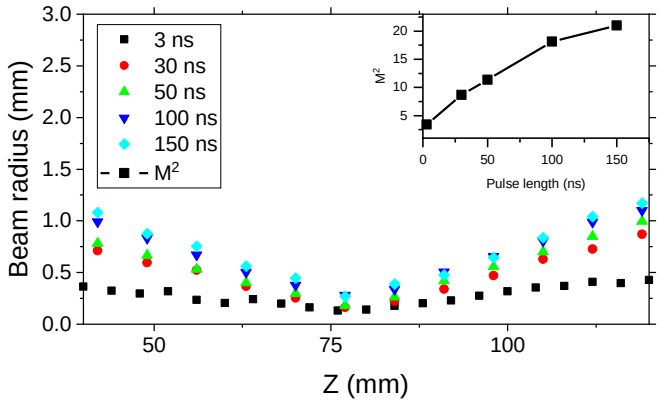

Figure 4. The effect of pulse length at a fixed pulse amplitude (20 A) and repetition frequency (5 kHz) on the caustic in the slow axis direction. The fitted M^2 value degradation with pulse length is shown in the inset.

The available lasers were then measured for the beam quality. A summary of the results is shown in Figure 5. There is a large improvement over QW based taper (variant F) with similar Γ and device geometry. Variant E, which was only an index guided RWG, showed low maximum power (<1 W), but nearly diffraction limited beam quality. The best beam quality out of the tapered devices is achieved with the variant D, which had a shorter (2 mm) taper section with a broader (3 degrees) opening angle than the variant B, which gave the highest output power. Variant B was only measured with longer (50 ns) pulses, and due to its mounting configuration (it was mounted on a heatsink) it was incompatible with the short pulse driver. However, we estimate, based on Figure 4, that its beam quality would have significantly improved in the short pulse regime. This estimate is also shown in Figure 5. This estimate should be considered cautiously, because there may be other detrimental effects from the longer and narrower taper in the gain-guided mode, which are neglected by this estimation. Variant C, with same design as B but with separate contacts (i.e. 30 µm absorption section between RWG and taper) showed a much lower output power. The device also showed no narrow pulse regime like variant D. This might be due to two effective absorption regions in the laser: one between the RWG and taper and another at the output facet. The shorter taper variants were cleaved from a long taper bar, and hence were missing this output passive section.

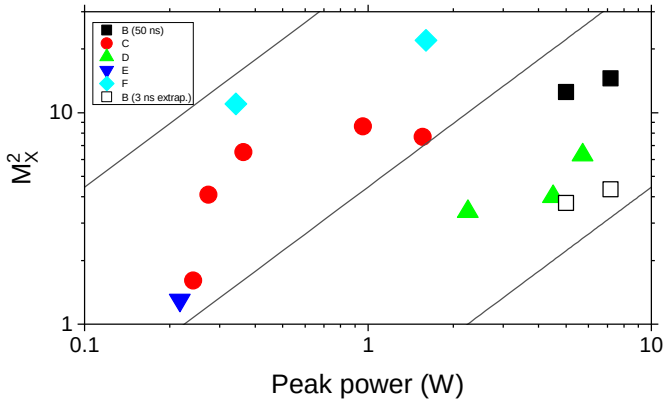

Figure 5. Measured slow axis M^2 values from the studied device variants at different output power levels. Constant brightness lines are shown for reference. The beam quality of variant B has been extrapolated to 3 ns pulse width using data from Figure 4.

More generally the results show that regardless of the pulsed pumping scheme, a gain-guided taper does not provide near diffraction-limited output. As shown by the RWG result, it can be improved with good index guiding, which has also been demonstrated recently with slightly different tapered variants [3]. We believe that the epilayer structure used here is well suitable for smaller lateral dimensions in the taper, as the saturation current density is in the $100\ \mathrm{kA/cm^2}$ range as measured for the RWG laser here. Smaller dimensions would also benefit the current input circuitry.

5. SUMMARY

We have characterized and analyzed tapered RWG lasers fabricated from a highly asymmetric bulk gain epilayer structure, capable of high peak powers. Different device geometries were compared against each other and to RWG device and a tapered device fabricated using a reference MQW epilayer. The results indicate that an absorption section inside the tapered cavity can decrease the pulse width, but at the same time reduces the maximum output peak power. The effect of pump current pulse length to both the LI and beam quality characteristics was demonstrated. Future work is needed to develop the lateral design to improve the beam guiding properties of the lasers and to establish optimal contacting and the possible position of the absorber region on the laser diode.

REFERENCES

[1] S. Kurtti, J.-P. Jansson, and J. Kostamovaara, "A CMOS Receiver–TDC Chip Set for Accurate Pulsed TOF Laser Ranging," *IEEE Transactions on Instrumentation and Measurement*, vol. 69, no. 5, pp. 2208–2217, May 2020, doi: 10.1109/TIM.2019.2918372.

[2] A. Knigge *et al.*, "Wavelength-Stabilized High-Pulse-Power Laser Diodes for Automotive LiDAR," *physica status solidi (a)*, vol. 215, no. 8, p. 1700439, 2018, doi: 10.1002/pssa.201700439.

[3] A. Zeghuzi, H. Christopher, A. Klehr, J.-P. Koester, H. Wenzel, and A. Knigge, "High-Brightness Nanosecond-Pulse Operation From Tapered-Ridge-Waveguide Lasers," *IEEE Photonics Technology Letters*, vol. 33, no. 3, pp. 151–154, Feb. 2021, doi: 10.1109/LPT.2020.3047150.

[4] S. Slipchenko *et al.*, "High-power pulsed (100 ns) laser sources (900 nm) based on epitaxially integrated heterostructures with tunnel p-n junctions," in *2021 27th International Semiconductor Laser Conference (ISLC)*, Oct. 2021, pp. 1–2. doi: 10.1109/ISLC51662.2021.9615693.

[5] L. W. Hallman *et al.*, "High Power 1.5μ m Pulsed Laser Diode With Asymmetric Waveguide and Active Layer Near p-cladding," *IEEE Photonics Technology Letters*, vol. 31, no. 20, pp. 1635–1638, Oct. 2019, doi: 10.1109/LPT.2019.2940231.

[6] B. Ryvkin, E. A. Avrutin, and J. T. Kostamovaara, "Asymmetric-Waveguide Laser Diode for High-Power Optical Pulse Generation by Gain Switching," *Journal of Lightwave Technology*, vol. 27, no. 12, pp. 2125–2131, Jun. 2009, doi: 10.1109/JLT.2008.2009075.

[7] B. S. Ryvkin, E. A. Avrutin, and J. T. Kostamovaara, “Asymmetric-waveguide, short cavity designs with a bulk active layer for high pulsed power eye-safe spectral range laser diodes,” *Semicond. Sci. Technol.*, vol. 35, no. 8, p. 085008, Jul. 2020, doi: 10.1088/1361-6641/ab8fbe.

[8] E. A. Avrutin and B. S. Ryvkin, “Travelling wave analysis of high pulsed power long-wavelength asymmetric-waveguide short-cavity laser diodes with a bulk active layer,” in *2021 International Conference on Numerical Simulation of Optoelectronic Devices (NUSOD)*, Sep. 2021, pp. 83–84. doi: 10.1109/NUSOD52207.2021.9541511.

[9] A. T. Aho, J. Viheriälä, M. Koskinen, T. Uusitalo, J. Reuna, and M. Guina, “High-Power 1.5 µm Tapered Distributed Bragg Reflector Laser Diodes for Eye-Safe LIDAR,” *IEEE Photonics Technology Letters*, vol. 32, no. 19, pp. 1249–1252, Oct. 2020, doi: 10.1109/LPT.2020.3019845.

[10] B. Lanz, B. S. Ryvkin, E. A. Avrutin, and J. T. Kostamovaara, “Performance improvement by a saturable absorber in gain-switched asymmetric-waveguide laser diodes,” *Opt. Express, OE*, vol. 21, no. 24, pp. 29780–29791, Dec. 2013, doi: 10.1364/OE.21.029780.

[11] D. Mehuys, L. Goldberg, and D. F. Welch, “5.25-W CW near-diffraction-limited tapered-stripe semiconductor optical amplifier,” *IEEE Photonics Technology Letters*, vol. 5, no. 10, pp. 1179–1182, Oct. 1993, doi: 10.1109/68.248420.